ELSEVIER

Palaeogeography, Palaeoclimatology, Palaeoecology 183 (2002) 247–260

PALAEO

www.elsevier.com/locate/palaeo

History of the South Java Current over the past 80 ka

Franz X. Gingele [a,c,*], Patrick De Deckker [a], Aurélie Girault [b], François Guichard [b]

[a] *Australian National University, Department of Geology, Canberra, ACT 0200, Australia*
[b] *LSCE, CNRS-CEA, Domaine du CNRS, 91198 Gif-sur-Yvette Cedex, France*
[c] *Baltic Sea Research Institute, Seestrasse 15, 18119 Rostock-Warnemuende, Germany*

Received 10 January 2001; accepted 27 November 2001

Abstract

A sediment core located below the present South Java Current (SJC) was used to reconstruct paleoclimate and paleoceanography on the basis of biogenic and terrigenic proxy-records. The core spans the past 80 ka of environmental change and shows considerable contrasts from the glacial to the Holocene. Presently, the core site is situated beneath a seasonally varying low-salinity tongue which is advected from the Java Sea via the Sunda Strait. It carries terrigenous matter of a characteristic signature. During the last glacial period (stage 4-2), when sea level was lower than during the Holocene, the Sunda Strait was closed and the terrigenous supply from that source ceased. As the core site is close to the equator, our results indicate that atmospheric and oceanographic circulation was alternatively dominated by the Northern Hemisphere East Asian Monsoon system and the Southern Hemisphere Australian Monsoon system. Between 20 and 12 ka, the (Australian) SE Winter Monsoon reached its maximum and intensified the westward flowing SJC. Increased mixing of the surface waters led to a slight rise in paleoproductivity. A similar but much weaker situation prevailed from 74 to 70 ka. During most of the glacial period, from 70 to 20 ka, strong northeasterly winds associated with the East Asian Winter Monsoon intensified the Indian Monsoon Current and the eastward flowing SJC, and may have also carried dust across the equator to our core site. During this glacial phase, populations of the giant diatom *Ethmodiscus rex* were thriving and may indicate a reduced deep and intermediate thermohaline circulation at the site. The monsoonal system as we know it today, with distinct dry and wet seasons, may not have been active before $\sim$12 ka.

Keywords: South Java Current; clay minerals; monsoon; paleoceanography; glacial; Holocene; *Ethmodiscus rex*

1. Introduction

The region of the South Java Current (SJC) is characterized by high variability in current directions and salinities. The near-surface (<100 m) component of the SJC is reversing directions every 3 months, driven by semi-annually varying winds in the central and eastern equatorial Indian Ocean (Wijffels et al., 1996). Maxima in eastward flow are reached at the end of the NW monsoon in May and at the transition from SE to NW monsoon in November (Wijffels et al., 1996). Near the May maximum, salinities in the SJC

* Corresponding author. Tel.: +49-381-5197380; Fax: +49-381-5197352.
E-mail address: franz.gingele@io-warnemuende.de (F. X. Gingele).

0031-0182/02/$ – see front matter
PII: S0031-0182(01)00489-8

can be as low as 32‰ and extend down to 13°S. Runoff from Sumatra and Java, and advection of fresher Java Sea water through the Sunda Strait may be responsible for this low-salinity 'tongue' (Wijffels et al., 1996). In August/September, during the peak of the SE monsoon, the throughflow from the Pacific into the Indian Ocean through the Timor Passage and the Lombok Straits is at its maximum, the flow of the SJC is weak and its direction possibly westward from September to October (Wyrtki, 1961); it incorporates some of the throughflow water (Godfrey and Ridgway, 1985). However, with 34.2–34.4‰, the SJC is still fresher than the throughflow, possibly due to continuing advection of Java Sea water.

The deep component of the SJC, which extends down to 1000 m, carries relatively saline North Indian Central Water and maintains an eastward flow (Wijffels et al., 1996). Phytoplankton productivity in this part of the eastern Indian Ocean is low, except for an area south of Java, where weak seasonal upwelling brings nutrients to the sea surface (Wyrtki, 1962; Martinez et al., 1998).

However, the present oceanographic and climatic system may have been established rather recently and been active for only 10 ka (De Deckker et al., 2002), whereas for most of the past 80 ka conditions were dramatically different. Sea level was substantially lower, not only during the last glacial maximum (LGM), but for most of the past 80 ka (Chappell et al., 1996), thus exposing huge shelf areas in the Indonesian Archipelago, and consequently affecting the heat and moisture exchange in the entire region. The throughflow from the Pacific to the Indian Ocean would have been maintained in the past, but the volume of throughflow was greatly restricted, with potential repercussions on the Global Thermohaline Circulation. Results from marine as well as continental climate records indicate that precipitation in the Indonesian Archipelago (van der Kaars, 1991, 1998; van der Kaars and Dam, 1995; De Deckker et al., 2002) and in northern Australia (Torgersen et al., 1988) was greatly reduced during the last glacial, resulting in a more saline throughflow (Martinez et al., 1997) and decreased runoff from the Indonesian Islands.

Synchronism of paleoclimatic events in the Northern and Southern Hemisphere has been discussed extensively on the basis of various continental and marine paleoclimate proxies. Although the matter is not yet resolved entirely, more and more evidence emerges that the atmospheric circulation intricately links both hemispheres, but may lead to different paleoclimatic records at individual sites (e.g. An, 2000). In our investigation area, there is evidence from modern meteorological data and paleoclimate records that the East Asian Monsoon and the Australian Monsoon system are linked by transequatorial air streams (An, 2000). Intensification of either the Siberian or Australian high enhances the (East Asian) Winter Monsoon or southeast (austral) Summer Monsoon, respectively, which in turn bring heat and vapor across the equator to the opposite hemisphere and influence precipitation in the respective wet seasons (An, 2000).

Deep-sea core BAR9442 is located close to the equator below the path of the present SJC and provides a continuous record of the past 80 ka. Biogenic and terrigenic proxies are used to decipher changes in current directions and properties of the involved water masses and construct a conclusive paleoceanographic and paleoclimatic scenario.

2. Materials and methods

Core BAR9442 was recovered during the 1994 BARAT campaign with the RV *Baruna Jaya I* from 2542 m water depth at 6°04.56′S and 102°25.08′E. The core consists of 9.8 m of mud with foraminifera-bearing sections, two defined ash layers at 5.39 m and 8.07–8.12 m (Figs. 1 and 2), and a sandy, water-rich zone at 6.5–7.1 m. This zone was probably disturbed during the coring procedure. The piston core and the associated trigger core were sampled at 10-cm intervals.

Sediment samples were treated with hydrogen peroxide (10%) and sieved over a 63-μm mesh. *Globigerinoides ruber* was hand picked from the fraction >63 μm and used for oxygen and carbon isotope measurements with a Finnigan MAT 251 at LSCE/CNRS, Gif-sur-Yvette.

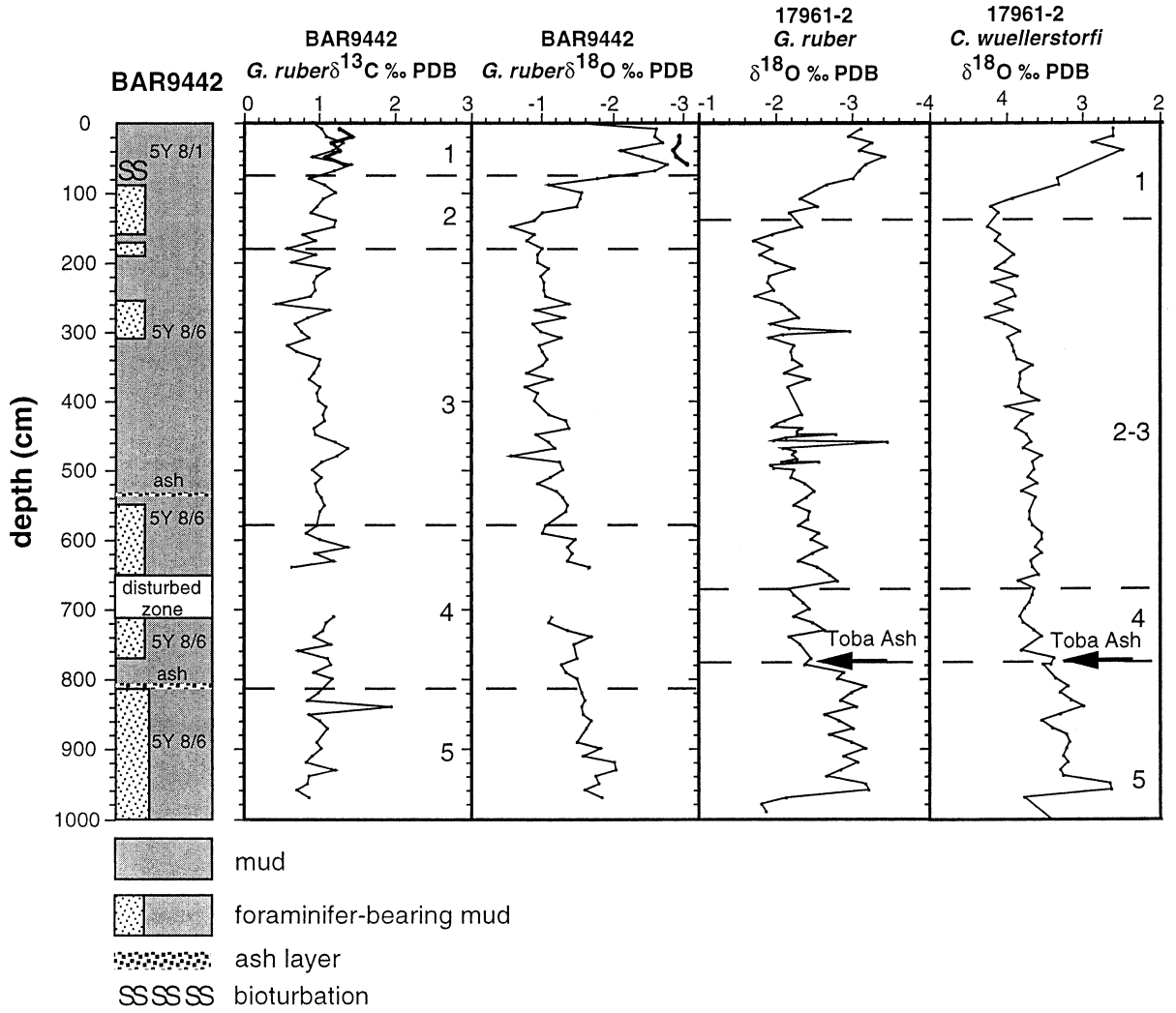

Fig. 1. Lithology, carbon- and oxygen-isotope records (*Globigerinoides ruber*) of core BAR9442. Short solid lines are carbon- and oxygen-isotope records of the trigger core. Isotope stages 5–1 are indicated. For comparison planktonic and benthonic oxygen-isotope records from core 17961-2 from the South China Sea, which have a similar resolution (Wang et al., 1999; for position see Fig. 4), are shown. Isotope stages and position of the Toba ash in this core after Bühring and Sarnthein (2000).

Clays were analyzed by adding acetic acid (10%) to the fraction < 63 μm to remove carbonate. Subsequently, it was split into silt (2–63 μm) and clay (< 2 μm) fractions by conventional settling techniques. The clay fraction was analyzed by X-ray diffraction (XRD; CoK_α radiation) for the four main clay mineral groups kaolinite, smectite, illite and chlorite following standard procedures developed by Biscaye (1965) and described in detail by Petschick et al. (1996). Contents of each clay mineral group in the sample are expressed as relative percentage. Quartz/feldspar ratios were calculated by using the integrated peak areas of the 4.26-Å quartz peak $\times 3$ divided by the combined area below the 3.18–3.24-Å feldspar peaks.

Carbonate was measured on dry bulk samples using a standard titration method. Samples were

dissolved in 1.1 mol/l HCl and titrations were conducted by using Metrohm Ion analysis, 716 DMS Titrino series 6.0 and AG CH-9101 pH meter. NaOH with a concentration of 0.5 mol/l was used as a base and three standards, consisting of 100% carbonate, were run after a batch of six samples to correct instrument drift.

The abundance of the giant diatom *Ethmodiscus rex* in the fraction >63 μm, which can be rather expressed by the volume of the fraction than by the weight, was assessed by roughly estimating the volume of the fraction >63 μm in a glass vial, subdivided by six evenly spaced arbitrary markings.

3. Stratigraphy and age control

The age model of core BAR9442 is based on the 10-cm spaced $\delta^{18}O$ record of the planktonic foraminifera *Globigerinoides ruber*. Individual isotope events 2.0, 2.2, 3.3 and 5.1 were identified by comparison with the SPECMAP-stack and tagged with the respective ages of Martinson et al. (1987). The ages for 2.2 and 2.0 were converted to calendar years using the approach of Stuiver et al. (1998). A distinct ash layer with a sharp base was found in the core at 8.07–8.12 m depth, which is considered to be synchronous with the beginning of stage 4 in the isotope record. Chemical analysis of glass shards and pumice was performed by microprobe and gave ambiguous results. Some particles, especially pumice and a few glass shards, were similar in composition to published results from the youngest Toba eruption (Chesner, 1998), others were deficient in silica and alkali metals. Therefore the ash layer was not used as a stratigraphic marker.

Ages between the stratigraphic fixpoints were obtained by linear interpolation using the 'analyseries' software of Paillard et al. (1996). Ages for the last five samples in the core were extrapolated assuming a constant sedimentation rate in isotope stage 5. The base of the core terminates at 81.5 ka. Comparison of the $\delta^{18}O$ record of the piston core BAR9442 to the $\delta^{18}O$ values from the uppermost 70 cm of the trigger core, which is supposed to contain the sediment surface somewhat undisturbed, shows a lag between both records. The clay mineral data from the trigger core show a similar lag. A downward shift of the isotope and clay record of of the piston core of 20 cm gives a reasonable fit with the trigger core, implying that about 20 cm may be missing from the top of the piston core.

A core from the South China Sea (17691-2) recently published by Wang et al. (1999) possesses a very similar sedimentation rate to BAR9442 and contains the distinct Toba ash layer at 7.8 m (8.1 m in BAR9442) (Bühring and Sarnthein, 2000). Further confirmation of our age model comes from the comparison of the $\delta^{18}O$ record in our core with that of Wang et al. (1999) (Fig. 1). Apart from a few freshwater spikes in the 17961-2 planktonic record, a striking similarity to BAR9442 is obvious (Fig. 1).

4. Biogenic proxies

Biogenic components in marine sediments can provide proxy-data on paleoproductivity and nutrients, ocean chemistry and circulation, sea-surface temperatures and salinity (for a comprehensive summary see Fischer and Wefer, 1999). The $\delta^{18}O$ and $\delta^{13}C$ record of the planktonic foraminifera *Globigerinoides ruber*, bulk carbonate content and the abundance of the giant diatom *Ethmodiscus rex* were available for interpretation in core BAR9442

The $\delta^{18}O$ record of *Globigerinoides ruber* shows the typical global glacial–interglacial shift, which was used to obtain an age model. It lacks rapid fluctuations during stages 2 and 3, which were observed in core 17961-2 by Wang et al. (1999) in the South China Sea and interpreted as 'freshwater' pulses at the sea surface. The glacial values (stage 2-4) in BAR9442 are on an average 1‰ heavier than in core 17961-2 from the South China Sea. It can be concluded that the area of the SJC was more saline than the South China Sea during the glacial period. It is likely that the closure of the Sunda Strait, drainage of the Sunda shelf to the North and increased salinity of the Indonesian Throughflow Water are responsible for this effect. Substantial reduction in pre-

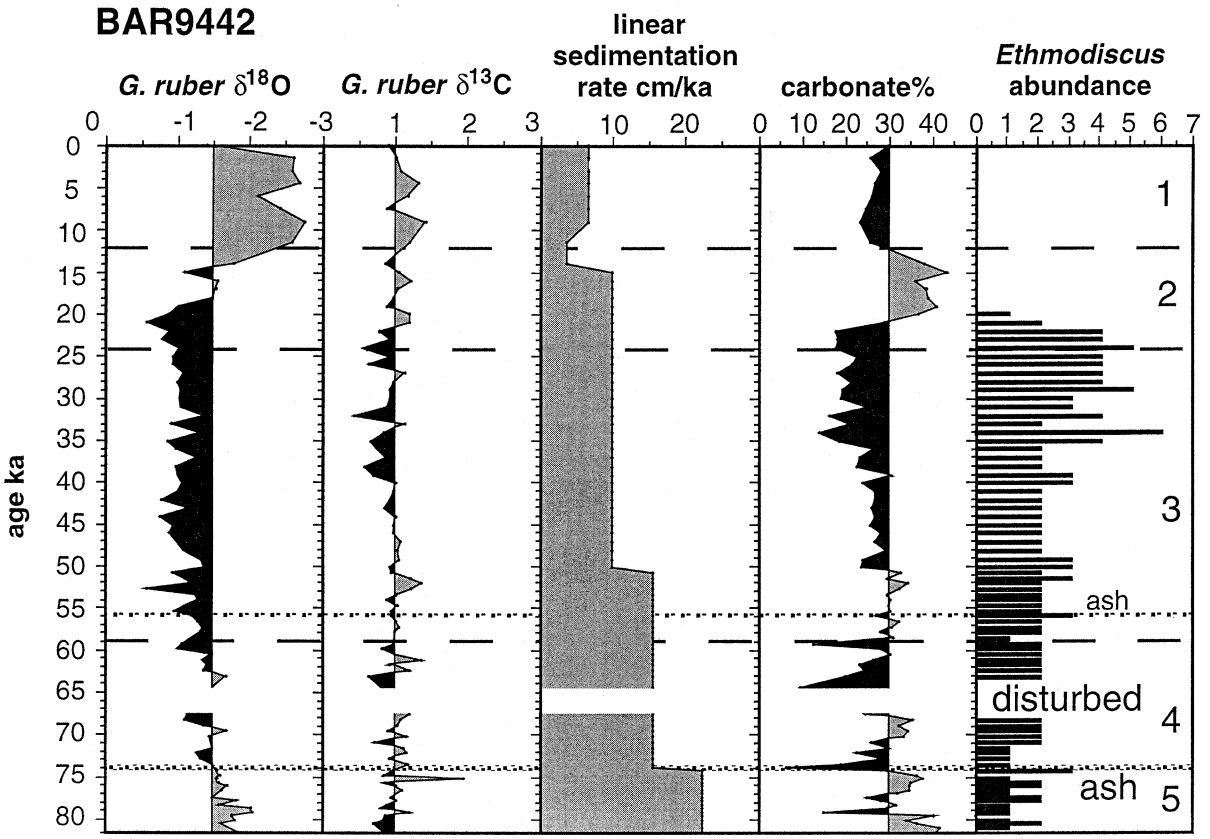

Fig. 2. Oxygen- and carbon-isotope records (*Globigerinoides ruber*), linear sedimentation rate, bulk carbonate and abundance of *Ethmodiscus rex* in core BAR9442 against age. Isotope stages 5–1 are indicated.

cipitation in the SE Asian region during the glacial further contributed to the increased sea-surface salinities (De Deckker et al., 2002).

The $\delta^{13}C$ record of *Globigerinoides ruber* shows a typical pattern of low glacial and high Holocene values. *G. ruber* is the shallowest-dwelling of all planktonic foraminifera and is believed to record nutrient contents in the uppermost mixed layer (30 m) of the ocean (Mulitza et al., 1997). The maximum amplitude between the glacial and the Holocene values is 1‰, but on average the shift between the Holocene and the glacial period between 40 and 20 ka is only 0.5‰. The global glacial–Holocene $\delta^{13}C$ shift for tropical planktonic foraminifera ranges from 0.2 to 0.8‰ depending on the influence of southern water masses, e.g. Antarctic Intermediate Water (Mulitza et al., 1999; Lea et al., 1999). Hence, the $\delta^{13}C$ variation in BAR9442 can be explained by the global glacial–Holocene shift alone. It is not only not necessary to assume increased nutrient levels and productivity in the uppermost mixed layer during the glacial, but also not consistent with the autecology of *Ethmodiscus rex* (see below).

Bulk carbonate shows minima in isotope stage 1, between 40 and 20 ka, and in the ash layers at 74 ka. Maxima occur well pronounced between 20 and 12 ka and in late stage 5. Carbonate deposition is a function of dissolution as well as production. Carbonate dissolution is controlled by water depth, bottom water chemistry and carbonate flux (Archer, 1991). Maxima in carbonate accumulation during the LGM and deglaciation were interpreted as a slight increase in glacial productivity in the eastern Indian Ocean (McCorkle et al., 1994; Martinez et al., 1998), and near the Timor

Trough (Müller and Opdyke, 2000). In some cores, the interpretation has been supported by independent proxies such as planktonic foraminifera assemblages or excess (biogenic) Ba accumulation (Müller and Opdyke, 2000).

As site BAR9442 is close to the foraminiferal lysocline of 2400 m, as suggested by Martinez et al. (1998), improved carbonate preservation during the LGM and the deglaciation is also a potential mechanism to explain the maximum in bulk carbonate. Due to its depth there is no indication of improved preservation during deglaciation in BAR9442, as suggested by a characteristic pteropod spike in cores from the western Pacific and the South China Sea. A high flux of organic carbon to the seafloor, associated with the sedimentation of *Ethmodiscus rex* populations, may have fostered carbonate dissolution at the sediment–water interface (Emerson and Bender, 1981). The termination of this organic carbon flux may have favored carbonate preservation. However, *E. rex* is also absent from stage 1, when carbonate values drop again.

A possible scenario emerges if viewed in context with our last biogenic proxy, the abundance of *Ethmodiscus rex*.

The occurrence and enrichment of the giant diatom *Ethmodiscus rex* (Wiseman and Hendey, 1953) in various marine sediment cores (Gardner and Burckle, 1975; Mikkelsen, 1977; Bjørklund and Jansen, 1984) have been regarded until recently as a mere curiosity. Ecophysiological investigations on *E. rex* and other deep-dwelling diatoms (Villareal, 1993; Villareal et al., 1993; Villareal and Carpenter, 1994; Pike and Kemp, 1999; Yoder et al., 1994; Kemp et al., 1999), and the discovery of extensive *E. rex* deposits in the Atlantic (Stabell, 1986; Abrantes et al., 1994; Gingele and Schmieder, 2001) and the Indian Ocean (Broecker et al., 2000) have focussed new attention on the behavior, autecology and paleoceanographic significance of *E. rex*. As *E. rex* is rarely found in surface plankton samples today, and is regarded as a character species of oligotrophic seas (Villareal, 1993), the formation of mass accumulation in sediments has long remained an enigma. Recent investigations have found deep-dwelling populations of *E. rex* near the nutricline (Villareal, 1993). The ability of active vertical migration of *E. rex* to utilize deep nitrogen pools has been interpreted as an adaptation to nutrient-poor seas (Villareal and Carpenter, 1994) and is especially efficient in stratified stable systems (Villareal, 1993).

Ethmodiscus rex is present in core BAR9442 from 80 to 20 ka with a pronounced maximum between 35 and 20 ka. It is absent from stage 1 and also during deglaciation and the later part of the LGM, periods when a strong bulk carbonate maximum occurs. The combination of an *E. rex* layer followed by a strong carbonate maximum has been found in mid-Pleistocene sediments of the Atlantic (Gingele and Schmieder, 2001) and has been interpreted as a consequence of reduced thermohaline circulation, followed by the subsequent onset of more turbulent conditions. A similar scenario may be applicable to BAR9442. A reduction of deep and intermediate circulation and a more stratified water column during the last glacial period, in particular between 35 and 20 ka could have trapped nutrients in deeper water masses, which were then utilized by populations of *E. rex*. The onset of more turbid conditions at 20 ka may have been supported by strong 'glacial' winds, reaching maximum strength during the late LGM, that would have recirculated nutrients to the surface and fostered nannoplankton productivity and zooplankton (foraminifera) abundance, as well as carbonate preservation. Still, it remains unclear why such an event is not paralleled by a shift in the $\delta^{13}C$ record. The use of an independent productivity proxy could solve the question if productivity or preservation was the main cause for the carbonate maximum during the late LGM and deglaciation period.

5. Terrigenic proxies

Clay minerals, quartz and feldspar concentrations in marine sediments provide terrigenic proxy-data, which can be used to decipher either climate changes in the source area on land, changes in the intensity of the input media (wind or rivers) or changes in ocean currents

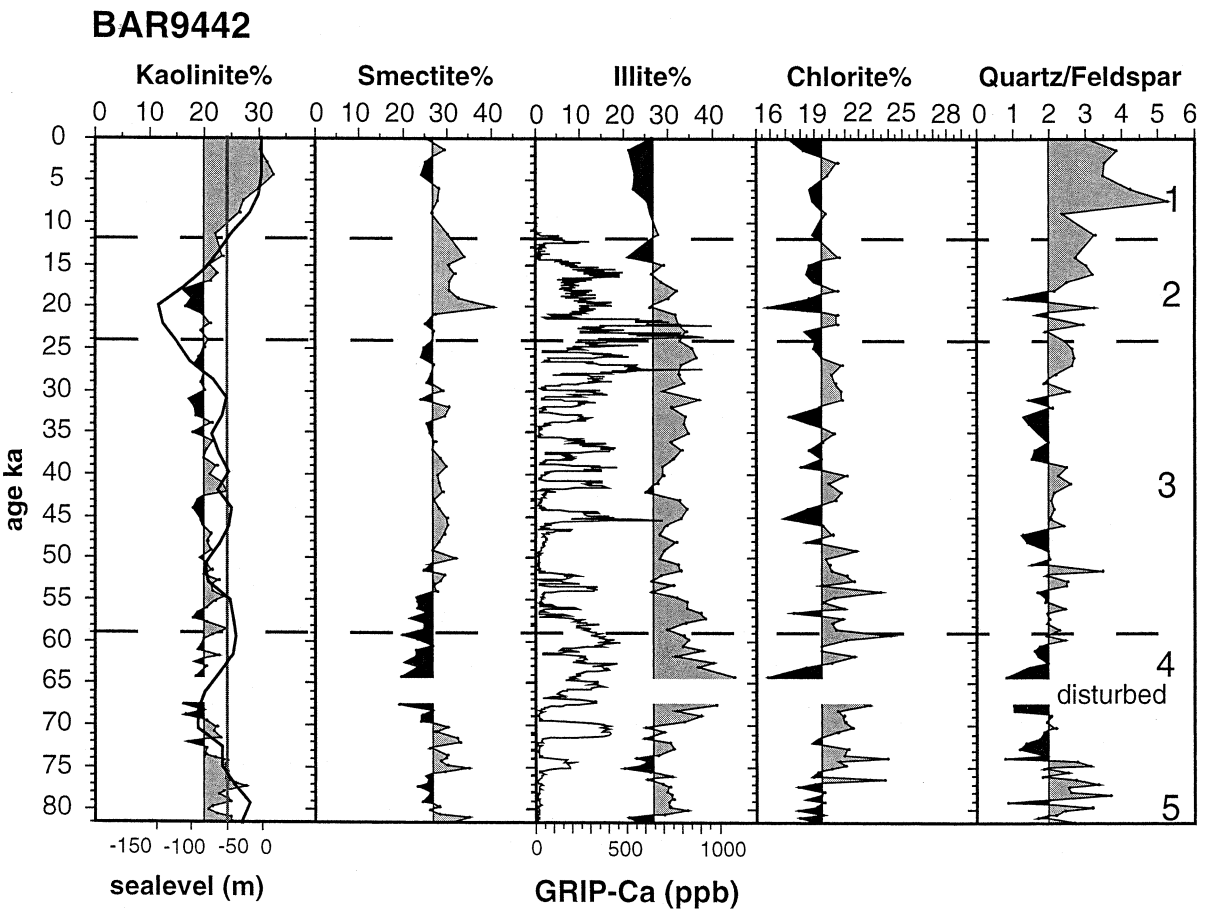

Fig. 3. Clay mineral percentages and quartz/feldspar ratios in core BAR9442. The downcore record of kaolinite is overlain by the global sea level curve of Chappell et al. (1996). The straight line delineates a sea level of −50 m, a threshold above which substantial amounts of kaolinite reach site BAR9442 after the Sunda Strait reopened. The GRIP Ice Core Ca record, representative for Northern Hemisphere dust propagation, is plotted onto the illite record of BAR9442 for comparison. Isotope stages 5–1 are indicated.

propagating the terrigenous input. The interpretation of downcore changes in mineral concentrations depends on the best possible information on modern distribution, sources and independent climate proxy-data in the source area. A comprehensive and detailed study on the clay mineral distribution and sources in the Indonesian Islands Arc and NW Australia was recently completed (Gingele et al., 2001) and is used as a basis for the interpretation of downcore records in core BAR9442.

Core site BAR9442 is situated on a submarine rise on the continental slope offshore southern Sumatra. Therefore, we believe that long-distance advection of clays within a nepheloid layer, frequently associated with circulation of bottom waters (e.g. Antarctic Bottom Water), is negligible for our site. Presently, site BAR9442 is bathed in Indian Deep Water (IDW), which represents that fraction of North Atlantic Deep Water (NADW) which is not converted into Intermediate Water in the Atlantic sector, but carried across the Indian Ocean with the upper Circumpolar Current (Tomczak and Godfrey, 1994). NADW carries kaolinite over long distances in the Atlantic (Petschick et al., 1996), implying that some of it could

theoretically reach site BAR9442. However, in the Circumpolar Current, the NADW clay mineral signature is quickly altered due to admixture of other clay minerals, such as chlorite in particular (Petschick et al., 1996). For this reason and due to the proximity of a strong local kaolinite source, we assume that long-distance transport of clays entrained in IDW is of minor importance for site BAR9442.

Kaolinite concentrations fluctuate around 20% throughout most of the glacial section of the core. Only in late isotope stage 5 and in the Holocene, kaolinite percentages increase to 25–35%. The reason for this feature is easy to explain, if viewed in the context of modern clay mineral distribution in the area (Gingele et al., 2001). Today, a kaolinite maximum is observed in the Sunda Strait. Low-salinity water from the Java Sea passes through the Sunda Strait and is injected into the SJC. Reversing directions semi-annually (Wijffels et al., 1996), the SJC transports any entrained kaolinite-rich, suspended matter eastward, but also westward to the site of core BAR9442. During the glacial, the Sunda Strait was dry, due to lowered sea level, which cut off the throughflow and the major source of kaolinite for site BAR9442. Plotting a global sea level curve (Chappell et al., 1996) on the kaolinite downcore record (Fig. 3) reveals that kaolinite percentages dropped sharply at 74 ka and increased substantially around 12–11 ka. These ages correspond to periods when the global sea level curve intersected the −45- to −50-m mark. The −50-m level is concurrent with the sill depth at the western entrance of the Sunda Strait. After sea level reached Holocene values again, a kaolinite maximum at 5 ka may represent a maximum influx of less saline Java Sea water.

Smectite percentages in the core fluctuate between 25 and 30%, which is consistent with other core-top samples in this region southwest of Sumatra (Gingele et al., 2001). Two distinct smectite maxima occur in the core with values of up to 35% at 75–70 ka and up to 40% from 20 to 12 ka. The only region where such high values can be observed today is the smectite-rich area south of Java, already described by Griffin et al. (1968), and an area south of Bali and Lombok (Gingele et al., 2001). As this is the only potential source for the high smectite values in core BAR9442, we assume that smectite was transported to the core site by the westward flowing SJC. The timing of the smectite peaks in core BAR9442 corresponds reasonably well to times of intense dune activity in Australia (Bowler, 1976), indicating maximum aridity and wind strength in the Southern Hemisphere during these periods. Intensification of the prevailing southeasterly winds, which result from a dominant anticyclone and a sharper pressure gradient over Australia during the glacial (Rognon and Williams, 1977), is likely to have intensified the surface component of the SJC. The concurrent possible weakening or absence of the monsoonal system during the LGM may have resulted in a near-permanent westward flow of the SJC and transport of the associated clays. If we follow this interpretation, a minimum in the downcore record of smectite between 70 and 55 ka could be interpreted as a weakening of the westward component of the SJC. A direct eolian influx of smectite between 75–70 and 20–12 ka is highly unlikely, as the potential dust sources in Australia and Central Asia (Chinese loess) have a different clay mineral composition. Kaolinite dominates dust from Australia (McTainsh, 1989), whereas illite is the major clay mineral in Chinese loess and smectite is virtually absent in both (Biscaye et al., 1997).

The illite record of BAR9442 is more difficult to interpret, since there are multiple potential sources. However, it is clear that during times of high sea level, when Sunda Strait remains open, illite-poor, terrigenous matter reaches the core site. Between 70 and 15 ka, illite values are higher, peaking between 70 and 55 ka, when smectite reaches a minimum. The modern distribution of clays in the area indicates two potential 'marine' source areas for the illites (Gingele et al., 2001). One is located near the eastern end of the Indonesian Islands Arc around Timor and in the Banda Sea, and the other at the northern tip of Sumatra. Transport of illite from Timor and the Banda Sea via the Indonesian Throughflow and subsequently the westward flowing SJC seems unlikely, because suspended matter would have to cross the smectite maximum south of Java and increased smec-

tite concentrations could be expected as well. As this is not the case, we assume that the illite maximum between 70 and 55 ka may result from a pronounced eastward flow of the deep and/or surface component of the SJC and associated transport of illite from the source near northern Sumatra. The eastward flow of the SJC may have been enhanced by strong NW winds during the glacial. There is general agreement (summary in Wang et al., 1999) that the Asian monsoon system produced stronger NE winds (NW south of the equator) during the last glacial and raised considerable amounts of dust from the more arid Central Asian sources (as Chinese loess). Illite is the major clay mineral in Chinese loess and can be found in increased concentrations throughout the glacial period in Greenland ice cores (GISP2, Biscaye et al., 1997). Calcium concentrations in the GRIP Ice Core can be used as an index of dust propagation in the Northern Hemisphere (Fuhrer et al., 1993, 1999) (Fig. 3). Periods of high dust (Ca) input in the GRIP Ice Core occur from 70 to 55 ka and from 35 to 20 ka and correspond reasonably well to the illite maxima and smectite minima in BAR9442. Given the proximity to site BAR9442 and the favorable wind directions, it seems very likely that during the glacial, dust from Central Asian sources may have contributed to the increased illite levels in core BAR9442 between 70 and 20 ka. However, individual Ca peaks in the GRIP Ice Core and illite peaks in BAR9442 are difficult to match because of uncertainties in the age models involved. First, the oxygen-isotope record in the glacial period of BAR9442 is not very well defined and provides few 'stratigraphic' fixpoints. Thus, ages are interpolated over a long period, assuming constant sedimentation rates.

Chlorite values are rather constant throughout the core and fluctuate between 18 and 20%. As chlorite concentrations are rather uniform along the Indonesian Islands Arc (Gingele et al., 2001), the changes in oceanography discussed above would only insignificantly affect downcore distribution of chlorite at site BAR9442. A major chlorite source in Sumatra is detected by high chlorite contents in sediments NW of BAR9442. Although there are strong indications that the Summer Monsoon was much weaker or absent during the glacial, and precipitation reduced by 30–70% (van der Kaars, 1991; De Deckker et al., 2002), some fluvial runoff must have persisted $\pm 5°$N and S of the equator (Wang et al., 1999). The uniform chlorite record at site BAR9442 may therefore represent a continuing supply with runoff from Sumatra.

Quartz/feldspar ratios are less distinct but, in general, mirror the kaolinite record. High ratios are most likely associated with the highly weathered, feldspar-poor kaolinite deposits in the Sunda Strait (Gingele et al., 2001).

6. Paleoceanographic reconstruction

6.1. 81–74 ka (isotope stage 5/4 transition)

Since our record commences at 81 ka, sea levels were already well below present values. The influx of Java Sea water, indicated by the kaolinite record, was restricted during late stage 5 and stopped completely after sea level dropped below -50 m. *Ethmodiscus rex* was present, although with low abundances, probably due to the reduction of thermohaline circulation and the availability of deep nutrient pools. A volcanic eruption at 74 ka deposited 5 cm of ash at our site. To date the origin of the ashes could not be identified. The same applies for the ash layer in a zone of water-rich sandy sediment in the core, equivalent to 67–65 ka, and another horizon at 56 ka.

6.2. 74–70 ka

The period from 74 to 70 ka coincides with times of increased windspeed in the Southern Hemisphere, and aridity (Wasson and Clark, 1988) in the Australasian region. Although the volume of the Indonesian Throughflow was reduced during the glacial, due to a low sea level, increased windspeed of the predominantly SE winds (Southern Hemisphere Winter Monsoon) from the Australian continent would have enhanced the velocity and pushed the Indonesian Throughflow waters further into the westward flowing SJC, thus explaining the smectite peak

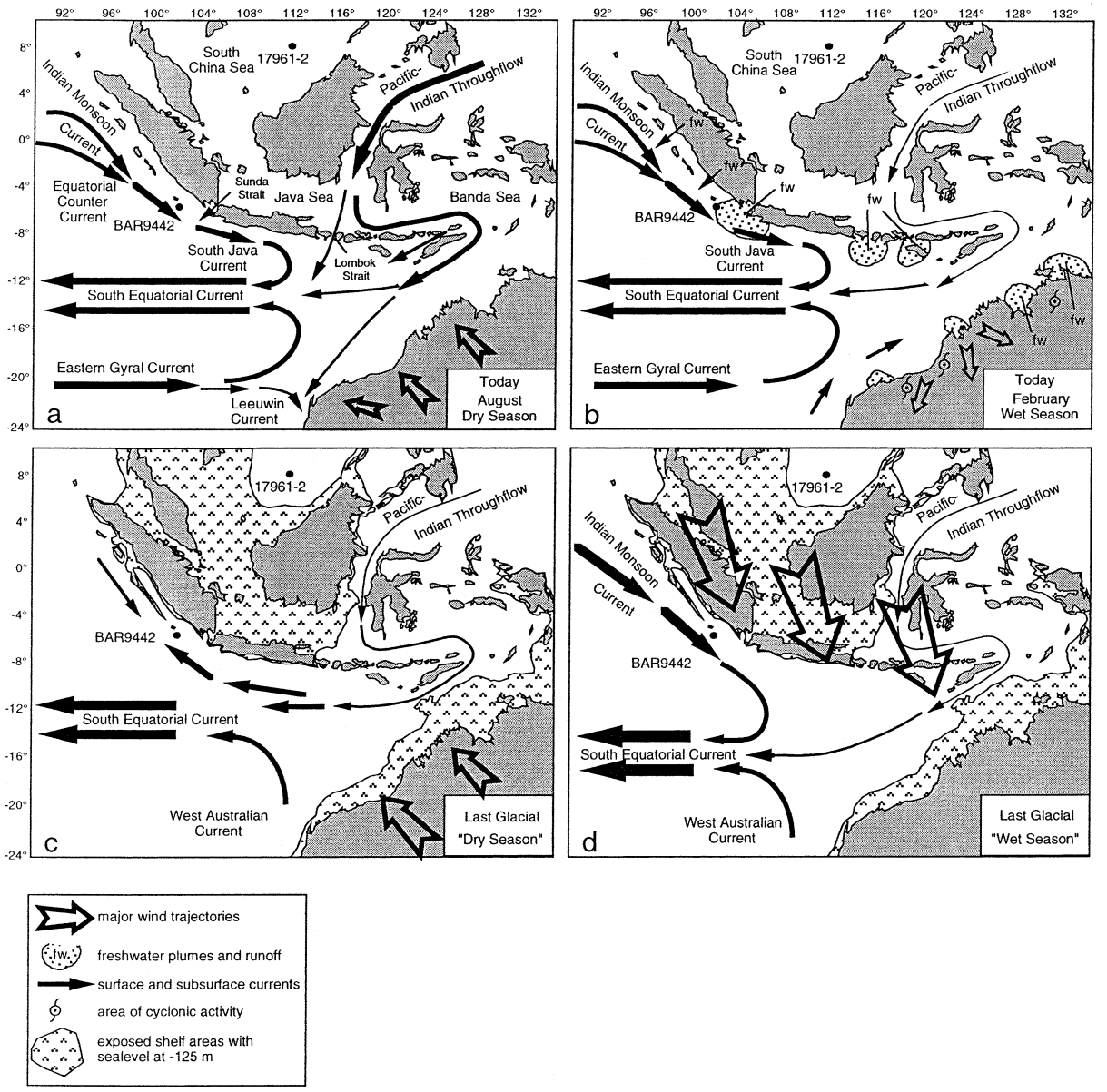

Fig. 4. Seasonally changing current and wind trajectories are depicted for today's wet (austral summer) and dry (austral winter) season and compared to two possible scenarios during the last glacial period.

at site BAR9442. *Ethmodiscus* abundance was reduced due to intensified circulation near the surface.

6.3. 70–35 ka

Little change is indicated by our proxies in the period from 70 to 35 ka. Properties of the water column were stable enough to support populations of *Ethmodiscus rex*, although only at moderate abundance. Following the interpretation of the smectite record the westward flow of the SJC and also the intensity of the Indonesian Throughflow were apparently slightly reduced from 70 to

55 ka. During this period, the eastward flow of the SJC, carrying illite and possibly some chlorite, was enhanced. Presently, the eastward flowing SJC is composed of a shallow, less saline layer and a deep component carrying North Indian Central Water. As there was no influx of less saline Java Sea water during this period it seems likely that the eastward flowing SJC was a uniform water mass. Although the climate was generally drier during the glacial some runoff must have persisted in northern Sumatra, which would have injected illite into the Indian Monsoon Current (Fig. 4) and the eastward flowing SJC. As the former is driven by the NW (boreal winter) monsoon, stronger northwesterly winds induced by a strong Siberian high during the glacial would have enhanced its flow. The correspondence of the GRIP Ca record with the illite record in BAR9442 in particular between 70 and 55 ka suggests that illite may have been also deposited directly with dust from Central Asia. This will require additional confirmation from the isotopic composition (Sr, Nd) of the clay components.

6.4. 35–20 ka

A sharp increase in *Ethmodiscus rex* abundance and reduction in carbonate are characteristic for this period and point to a maximum in stratification of the water column. Low smectite percentages indicate a minimum in the westward flowing SJC and the Indonesian Throughflow. The reduced thermohaline circulation was dominated by the saline North Indian Central Water advected with an eastward flowing SJC. High illite concentrations, induced either as dust with the NW monsoon or with the Indian Monsoon Current and eastward flowing SJC, point to the persistence of northwesterly wind directions.

6.5. 20–12 ka

The period from 20 to 12 ka incorporates the late LGM and the subsequent deglaciation. Climate conditions during the LGM in the Southern Hemisphere are similar to the period from 74 to 70 ka and may have been even more extreme. Windspeeds and aridity in the Australasian region were high as indicated by dune building activity in the Australian interior, which lasted from the LGM well into the deglaciation (Wasson, 1986). A strong smectite peak from 20 to 18 ka at site BAR9442 suggests a maximum in the westward flowing SJC, and the incorporation of the Indonesian Throughflow into the SJC. The intertropical convergence zone (ITCZ) was fully in place well after the glacial maximum, indicating strengthening of the SE monsoon (De Deckker et al., 1991). In contrast to most of the glacial period, site BAR9442 was influenced by Southern Hemisphere winds between 20 and 12 ka. *Ethmodiscus rex* populations disappear completely from the record, whereas carbonate reaches a maximum, indicating the onset of more turbid conditions in the water column. It is interesting to note that, although the strong SE monsoon influenced site BAR9442 via the surface ocean circulation, a direct influx of dust from Australia, which consists predominantly of kaolinite (e.g. Griffin et al., 1968), could not be observed. This may be due to the westward directed dust trajectories (Bowler, 1976).

6.6. 12 ka–present (isotope stage 1)

Paleoceanographic conditions during this period were completely different from those of the previous 70 ka. The rising global sea level crossed the −50-m threshold, inundated the Sunda shelf and enabled throughflow of less saline Java Sea water through the Sunda Strait into the path of the SJC. This process is documented by the advection of kaolinite from the Sunda Strait. Populations of *Ethmodiscus rex* never re-established after 20 ka due to an onset of an effective deep circulation system.

7. Conclusions

The region of the SJC south of Sumatra experienced significantly different climatic and oceanographic conditions during the last glacial compared to today (Fig. 4). Today, the climate of the area is characterized by seasonal changes from the NW to the SE monsoon, which change directions

of the SJC accordingly and by a high amount of precipitation (Fig. 4a,b). Lower salinity surface water reaches the SJC via the Sunda Strait. The freshwater 'tongue' south of the Sunda Strait inhibits the advection of suspended matter with the Indian Monsoon Current from offshore northern Sumatra.

During the last glacial, global sea level was low and the input of low-salinity water and terrigenous matter via the Sunda Strait was cut off. Strong, northwesterly winds, induced by a strong Siberian high, were associated with the East Asian Winter Monsoon (February, Fig. 4d) and prevailed, in particular from 70 to 55 ka and from 35 to 20 ka. The scenario can be compared to a modern 'wet season' situation, but with considerable less rainfall in the equatorial region. The Indian Monsoon Current had probably intensified and, in the absence of a low-salinity tongue, illite-rich material could have been transported from near northern Sumatra to the South. It is also very likely that some illite was directly injected into the SJC with eolian dust from Central Asian sources. The South Equatorial Current system probably occupied a more southerly position than today and received the reduced volume of the Indonesian Throughflow during this glacial period.

During two distinct periods, from 74 to 70 ka and more obviously from 20 to 12 ka, Southern Hemisphere atmospheric circulation replaced the normally dominant Northern Hemisphere atmospheric circulation. Smectite was transported from south of Lombok, Bali and Java towards South Sumatra with a westward flowing SJC. This can only be achieved if a strong SE monsoon, similar to an extremely strong 'dry season' today, lowers the steric height in the Indian Ocean, accelerates the velocity (not necessarily the volume) of the Indonesian Throughflow and pushes the throughflow water into the westward flowing SJC (Fig. 4c). The ITCZ had shifted north and the aridity in Australia peaked during these two brief periods (Wasson, 1986; De Deckker et al., 1991), while humidity associated with the East Asian Summer Monsoon was increased and there was reduced dust availability from Central Asian sources.

Today, the investigation area is characterized by a strong seasonal climate with wet and dry periods (Fig. 4a,b). The 'seasonal' scenarios shown for the last glacial may not have been seasonal at all, but dominant during most of the year. Our proxy-data show that the 'dry season' situation may have prevailed from 74 to 70 and 20 to 12 ka, whereas the 'wet season' situation (NW monsoon, which was not that wet during the glacial) may have prevailed from 70 to 55 and 35 to 20 ka.

Acknowledgements

This project was supported by IREX-ARC Fellowship Grant No. X00001658 awarded to P.D.D. The laboratory assistance of G. Ott was greatly appreciated. We also thank B. Opdyke for help with the carbonate analysis. We are grateful to C.-D. Hillenbrand who performed the XRD analyses and to D. Blamart and R. Ouadhi for isotopic measurements. The efforts of K. Earle and R. Arculus in analyzing the ash layers are greatly acknowledged. Thanks are due to the master and crew of the RV *Baruna Jaya I*, who recovered the core in 1994. The BARAT cruise took place with the financial support of INSU (CNRS France), CEA, IFREMER and of the 'service culturel' of the French Embassy in Jakarta. Operations at sea were performed with the help of the Indonesian crew and three seamen from GENAVIR (IFREMER). Scientists from MGI (Bandung), BPPT and LIPI (Jakarta) are also acknowledged for their work at sea. The comments of S. van der Gaast, F. Surlyk and two anonymous reviewers greatly improved the manuscript. Thanks to them all.

References

Abrantes, F., Winn, K., Sarnthein, M., 1994. Late Quaternary Paleoproductivity variations in the NE and Equatorial Atlantic: diatom and Corg Evidence. In: Zahn, R., Pedersen, T.F., Kaminski, M.A., Labeyrie, L. (Eds.), Carbon Cycling in the Glacial Oceans. NATO ASI, Springer, Berlin, pp. 425–439.

An, Z., 2000. The history and variability of the East Asian paleomonsoon climate. Quat. Sci. Rev. 19, 171–187.

Archer, D., 1991. Equatorial Pacific calcite preservation cycles: Production or dissolution? Paleoceanography 6, 561–571.

Biscaye, P.E., 1965. Mineralogy and sedimentation of recent deep-sea clay in the Atlantic Ocean and adjacent seas and oceans. GSA Bull. 76, 803–832.

Biscaye, P.E., Grousset, F.E., Revel, M., van der Gaast, S., Zielinski, G.A., Vaars, A., Kukla, G., 1997. Asian provenance of glacial dust (stage 2) in the Greenland Ice Sheet Project 2 Ice Core, Summit, Greenland. J. Geophys. Res. 102, 26765–26781.

Bjørklund, K.R., Jansen, J.H.F., 1984. Radiolaria distribution in middle and late Quaternary sediments and paleoceanography in the eastern Angola Basin. Neth. J. Sea Res. 17, 299–312.

Bowler, J.M., 1976. Aridity in Australia: Age, origins and expressions in aeolian landforms and sediments. Earth Sci. Rev. 12, 279–310.

Broecker, W.S., Clark, E., Lynch-Stieglitz, J., Beck, W., Stott, L.D., Hajdas, I., Bonani, G., 2000. Late glacial diatom accumulation at 9°S in the Indian Ocean. Paleoceanography 15, 348–352.

Bühring, C., Sarnthein, M., 2000. Toba ash layers in the South China Sea: Evidence of contrasting wind directions during eruption ca. 74 ka. Geology 28, 275–278.

Chappell, J., Omura, A., Esat, T., McCulloch, M., Pandolfi, J., Ota, T., Pillans, B., 1996. Reconciliation of late Quaternary sea levels derived from coral terraces at Huon Peninsula with deep-sea oxygen isotope records. Earth Planet. Sci. Lett. 141, 227–236.

Chesner, C.A., 1998. Petrogenesis of the Toba Tuffs, Sumatra, Indonesia. J. Petrol. 39, 397–438.

De Deckker, P., Corrège, T., Head, J., 1991. Late Pleistocene record of cyclic eolian activity from tropical Australia suggesting the Younger Dryas is not an unusual climatic event. Geology 19, 602–605.

De Deckker, P., Tapper, N.J., van der Kaars, S., 2002. Ice age conditions for the Warm pool reassessed. Global Planet. Sci., in press.

Emerson, S., Bender, M., 1981. Carbon fluxes at the sediment–water interface of the deep-sea: Calcium carbonate preservation. J. Mar. Sci. 39, 139–162.

Fischer, G., Wefer, G., 1999. Use of Proxies in Paleoceanography: Examples from the South Atlantic. Springer, Berlin, pp. 1–735.

Fuhrer, K.E., Wolff, W., Johnsen, S., 1999. Timescales for dust variability in the Greenland ice core project (GRIP) in the last 100.000 years. J. Geophys. Res. 104 (D24), 31043–31052.

Fuhrer, K., Neftel, A., Anklin, M., Maggi, V., 1993. Continuous measurements of hydrogen peroxide, formaldehyde, calcium and ammonium concentrations along the new GRIP ice core from Summit, Central Greenland. Atm. Environ. 12, 1873–1880.

Gardner, J.V., Burckle, L.H., 1975. Upper Pleistocene Ethmodiscus rex oozes from the eastern equatorial Atlantic. Micropaleontology 21, 236–242.

Gingele, F.X., De Deckker, P., Hillenbrand, C.-D., 2001. Clay mineral distribution in surface sediments between Indonesia and NW Australia – source and transport by ocean currents. Mar. Geol. 179, 135–146.

Gingele, F.X., Schmieder, F., 2001. Anomalous South Atlantic lithologies confirm global scale of unusual mid-Pleistocene climate excursion. Earth Planet. Sci. Lett. 186, 93–101.

Godfrey, J.S., Ridgway, K.R., 1985. The large-scale environment of the poleward-flowing Leeuwin Current, Western Australia: Longshore steric height gradients, wind stresses and geostrophic flow. J. Phys. Oceanogr. 15, 481–495.

Griffin, J.J., Windom, H.L., Goldberg, E.D., 1968. The distribution of clay minerals in the World Ocean. Deep-Sea Res. 15, 433–459.

Kemp, A.E.S., Pearce, R.B., Koizumi, I., Pike, J., Rance, S.J., 1999. The role of mat-forming diatoms in the formation of Mediterranean sapropels. Nature 398, 57–61.

Lea, D.W, Bijma, J., Spero, H.J., Archer, D., 1999. Implications of a carbonate ion effect on shell carbon and oxygen isotopes for glacial ocean conditions. In: Fischer, G., Wefer, G. (Eds.), Use of Proxies in Paleoceanography: Examples from the South Atlantic. Springer, Berlin, pp. 513–522.

Martinez, J.I., De Deckker, P., Chivas, A.R., 1997. New estimates for salinity changes in the Western Pacific Warm Pool during the Last Glacial Maximum: oxygen-isotope evidence. Mar. Micropaleontol. 32, 311–340.

Martinez, J.I., Taylor, L.C., De Deckker, P., Barrows, T.T., 1998. Planktonic foraminifera from the eastern Indian Ocean and the southern boundary of the western Pacific Warm Pool (WPWP). Mar. Micropaleontol. 34, 121–151.

Martinson, D.G., Pisias, N.G., Hays, J.D., Imbrie, J., Moore, T.C., Shackleton, N.J., 1987. Age dating and the orbital theory of the ice ages: Development of a high-resolution 0–300,000-year chronostratigraphy. Quat. Res. 27, 1–29.

McCorkle, D.C., Veeh, H.H., Heggie, D.T., 1994. Glacial–Holocene paleoproductivity off western Australia: a comparison of proxy records. In: Zahn, R. et al. (Eds.), Carbon Cycling in the Glacial Ocean: Constraints on the Ocean's Role in Global Change. NATO ASI Ser. 117, pp. 443–479.

McTainsh, G.H., 1989. Quaternary aeolian dust processes and sediments in the Australian region. Quat. Sci. Rev. 8, 235–253.

Mikkelsen, N., 1977. On the origin of *Ethmodiscus* ooze. Mar. Micropaleontol. 2, 35–46.

Mulitza, S., Arz, H., Kemle-von Mücke, S., Moos, C., Niebler, H.-S., Pätzold, J., Segl, M., 1999. The South Atlantic carbon isotope record of planktic foraminifera. In: Fischer, G., Wefer, G. (Eds.), Use of Proxies in Paleoceanography: Examples from the South Atlantic. Springer, Berlin, pp. 427–445.

Mulitza, S., Niebler, H.S., Duerkoop, A., Wefer, G., 1997. Planktonic foraminifera as recorders of past surface water stratification. Geology 25, 335–338.

Müller, A., Opdyke, B.N., 2000. Glacial–interglacial changes in nutrient utilization and paleoproductivity in the Indone-

sian Throughflow sensitive Timor Trough, easternmost Indian Ocean. Paleoceanography 15, 85–94.

Paillard, D., Labeyrie, L., Yiou, P., 1996. Macintosh program performs time-series analysis. EOS 77, 379.

Petschick, R., Kuhn, G., Gingele, F.X., 1996. Clay Mineral Distribution in Surface Sediments of the South Atlantic – Sources, Transport and Relation to Oceanography. Mar. Geol. 130, 203–229.

Pike, J., Kemp, A.E.S., 1999. Diatom mats in the Gulf of California sediments: Implications for the paleoenvironmental interpretation of laminated sediments and silica burial. Geology 27, 311–314.

Rognon, P., Williams, M.A.J., 1977. Late Quaternary climatic changes in Australia and North Africa: A preliminary interpretation. Palaeogeogr. Palaeoclimatol. Palaeoecol. 21, 285–327.

Stabell, B., 1986. Variations of diatom flux in the eastern equatorial Atlantic during the last 400,000 years ('meteor' cores 13519 and 13521). Mar. Geol. 72, 305–323.

Stuiver, M., Reimer, P.J., Bard, E., Beck, J.W., Burr, G.S., Hughen, K.A., Kromer, B., McCormick, G., van der Plicht, J., Spurk, M., 1998. INTCAL98 radiocarbon age calibration, 24,000–0 cal BP. Radiocarbon 40, 1041–1083.

Tomczak, M., Godfrey, J.S., 1994. Regional Oceanography: an Introduction. Pergamon Press, Oxford.

Torgersen, T., Luly, J., De Deckker, P., Jones, M.R., Searle, D.E., Chivas, A.R., Ullman, W.J., 1988. Late Quaternary environments of the Carpentaria Basin, Australia. Palaeogeogr. Palaeoclimatol. Palaeoecol. 67, 245–261.

van der Kaars, S., 1991. Palynology of eastern Indonesian marine piston-cores: a late Quaternary vegetation and climatic record for Australasia. Palaeogeogr. Palaeoclimatol. Palaeoecol. 85, 239–302.

van der Kaars, S., 1998. Marine and terrestrial pollen records of the last glacial cycle from the Indonesian region: Bandung Basin and Banda Sea. Paleoclimates 3, 209–219.

van der Kaars, S., Dam, M.A.C., 1995. A 135,000-year record of vegetational and climatic change from the Bandung area, west Java, Indonesia. Palaeogeogr. Palaeoclimatol. Palaeoecol. 117, 55–72.

Villareal, T.A., 1993. Abundance of the giant diatom *Ethmodiscus* in the Southwest Atlantic Ocean and Central Pacific Gyre. Diatom Res. 8, 171–177.

Villareal, T.A., Altabet, M.A., Culver-Rymsza, K., 1993. Nitrogen transport by vertically migrating diatom mats in the North Pacific Ocean. Nature 363, 709–712.

Villareal, T.A., Carpenter, E.J., 1994. Chemical composition and photosynthetic characteristics of Ethmodiscus rex (Bacillariophyceae): evidence for vertical migration. J. Phycol. 30, 1–8.

Wang, L., Sarnthein, M., Erlenkeuser, H., Grimalt, J., Grootes, P., Heilig, S., Ivanova, E., Kienast, M., Pelejero, C., Pflaumann, U., 1999. East Asian monsoon climate during the Late Pleistocene: high-resolution sediment records from the South China Sea. Mar. Geol. 156, 245–284.

Wasson, R.J., 1986. Geomorphology and Quaternary history of the Australian continental dunefields. Geogr. Rev. Jpn. Ser. B 59, 55–67.

Wasson, R.J., Clark, R.L., 1988. The Quaternary in Australia – Past, present and future. Quat. Australas. 6, 17–22.

Wijffels, S.E., Hautala, S., Meyers, G., Morawitz, W., 1996. The WOCE Indonesian Throughflow Repeat Hydrography Sections: I10 and IR6. Int. WOCE Newsl. 24, 25–28.

Wiseman, J.D.H., Hendey, N.I., 1953. The significance and diatom content of a deep-sea floor sample from the neighbourhood of the greatest oceanic depth. Deep-Sea Res. 1, 47–59.

Wyrtki, K., 1961. Scientific results of marine investigations of the South China Sea and the Gulf of Thailand. NAGA Report 2, University of California, Scripps Institute of Oceanography, La Jolla, CA, pp. 1–195.

Wyrtki, K., 1962. The upwelling in the region between Java and Australia during the southeast-monsoon. Aust. J. Mar. Freshw. Res. 13, 217–225.

Yoder, J., Ackleson, S.G., Barber, R.T., Flament, P., Balch, W.M., 1994. A line in the sea. Nature 371, 689–692.